



A partially-coupled hydro-mechanical analysis of the Bengal Aquifer System under hydrological loading

Nicholas D. Woodman^{1†}, William G. Burgess¹, Kazi Matin Ahmed² and Anwar Zahid³

¹Department of Earth Sciences, University College London, London WC1E 6BT, UK, ²Department of Geology, Dhaka University, Dhaka 1000, Bangladesh, ³Bangladesh Water Development Board, Dhaka, Bangladesh, [†]current address: Faculty of Engineering and the Environment, University of Southampton, Southampton SO17 1BJ, UK

Correspondence to: Nicholas D Woodman (n.d.woodman@soton.ac.uk)

Abstract. The coupled poro-mechanical behaviour of geologic-fluid systems is fundamental to numerous processes in structural geology, seismology and geotechnics but is frequently overlooked in hydrogeology. Substantial poro-mechanical influences on groundwater head have recently been highlighted in the Bengal Aquifer System, however, driven by terrestrial water loading across the Ganges-Brahmaputra-Meghna floodplains. Groundwater management in this strategically important fluvio-deltaic aquifer, the largest in south Asia, requires a coupled hydro-mechanical approach which acknowledges poro-elasticity. We present a simple partially-coupled, one-dimensional poro-elastic model of the Bengal Aquifer System, and explore the poro-mechanical responses of the aquifer to surface boundary conditions representing hydraulic head and mechanical load under three modes of terrestrial water variation. The characteristic responses, shown as amplitude and phase of hydraulic head in depth profile and of ground surface deflection, demonstrate (i) the limits to using water levels in piezometers to indicate groundwater recharge, as conventionally applied in groundwater resources management; (ii) the conditions under which piezometer water levels respond primarily to changes in the mass of terrestrial water storage, as applied in geological weighing lysimetry; (iii) the relationship of ground surface vertical deflection to changes in groundwater storage; and (iv) errors of attribution that could result from ignoring the poroelastic behaviour of the aquifer. These concepts are illustrated through application of the partially-coupled model to interpret multi-level piezometer data at two sites in southern Bangladesh. There is a need for further research into the coupled responses of the aquifer due to more complex forms of surface loading, particularly from rivers.

1 Introduction

Throughout the Bengal Basin, the floodplains of the Ganges, Brahmaputra and Meghna (GBM) rivers (Fig. 1) are underlain by the Bengal Aquifer System (BAS), the largest aquifer in south Asia and the source of water to over 100 million people (Burgess et al., 2010). Management of the BAS groundwater resource relies on monitoring water levels in networks of



30 observation boreholes, taking the conventional approach that changes in groundwater heads represent volumetric changes in
31 groundwater storage through recharge and drainage (Shamsudduha et al., 2011). This approach presumes the hydraulic
32 behaviour of the aquifer to be decoupled from its mechanical response to changes in stress. Recently, however, the distinctively
33 poroelastic behaviour of the BAS has been recognised (Burgess et al., 2017), by which groundwater heads are subject to
34 substantial mechanical perturbation driven by changes in the mass of terrestrial water storage (TWS) above the surface of the
35 aquifer. A coupled hydro-mechanical approach is necessary for understanding groundwater conditions and managing resources
36 in this environment, particularly in relation to recharge (Shamsudduha et al., 2012), sustainability of groundwater abstraction
37 for irrigation (Shamsudduha et al., 2008) and municipal water supply (Ravenscroft et al., 2013), and the security of schemes
38 for mitigation against groundwater arsenic (Michael and Voss, 2008) and salinity (Rahman et al., 2011; Sultana et al., 2015).
39 The generally coupled poro-mechanical nature of geologic-fluid systems is well-established (Neuzil, 2003); porewater
40 pressures affect the stress state and vice-versa. These interactions are accepted as important where groundwater conditions are
41 related to faulting (Roeloffs, 1988; Rojstaczer and Agnew, 1989; Sutherland et al., 2017), earthquakes (Manga et al., 2012),
42 pumping-induced aquitard responses (Verruijt, 1969), ground subsidence (Burbey et al., 2006; Erban et al., 2014), glacial
43 loading effects (Bense and Person, 2008; Black and Barker, 2016) and surface water interactions (Acworth et al., 2015; Boutt,
44 2010). Use of ground surface vertical displacements to infer aquifer or groundwater conditions (Chaussard et al., 2014; Reeves
45 et al., 2014) is also predicated on coupling of the hydraulic and mechanical behaviour of aquifer sediments. For simulation of
46 transient groundwater flow in aquifers, however, a decoupling simplification is frequently applied such that the elastic equation
47 does not need to be solved simultaneously. Thus, the flow equation is solved without consideration of internal stresses and
48 strains or mechanical boundary conditions. Despite this, the poro-mechanical nature of confined aquifers is embedded in the
49 concept of specific storage which incorporates the elastic compressibility of the aquifer materials (Domenico and Schwartz,
50 1998; Green and Wang, 1990; Narasimhan, 2006). The decoupling assumption is reasonable where the effects of mechanical
51 loading can be considered insignificant, either when the changes in load are small, or when the applied load is mostly borne
52 by the solid rather than the fluid (Black and Barker, 2016). Neither of these conditions apply to the BAS sediments, which are
53 highly compressible (Steckler et al., 2010) and subject to substantial and extensive TWS mechanical loads due to heavy rainfall,
54 deep flooding and large river discharges as a consequence of the annual monsoon (Shamsudduha et al., 2012).
55 In the event of laterally-extensive changes to mechanical loads and/or hydraulic heads above the surface of an aquifer, and
56 laterally-homogeneous aquifer properties, by symmetry it may be deduced that lateral strains are zero. This condition gives
57 rise to a *partial* coupling of the elastic and fluid pressure equations (Neuzil, 2003). In the case of *partial* coupling, changes to
58 the mechanical load due to the changing mass of water near or at the surface may be included within the flow equation, one-
59 dimensionally in the vertical direction, and the solutions will satisfy all the equilibrium and compatibility requirements for
60 stress and strain. There is no need to solve the elastic equation in order to calculate pressures in the aquifer, although once the
61 flow equation is solved, the pressures can be substituted into the elastic equation to provide stresses and strains. A sub-set of
62 this partially-coupled condition occurs where there is negligible groundwater flow, due to very low hydraulic gradients, low
63 permeability or a combination of both. This can be the situation in extensive fluvio-deltaic aquifers of low topographic relief



such as the BAS (Burgess et al., 2017) if mechanical loading is imposed at the surface in a manner which does not induce significant vertical hydraulic gradients. Under these conditions, porewater pressures are determined by changes to surface mechanical loading alone, and changes in groundwater head may be taken as a measure of changes in TWS mechanical loading above the surface of the aquifer. This is the conceptual basis for geological weighing lysimetry (Bardsley and Campbell, 2007, 1994; van der Kamp and Schmidt, 1997, 2017) as used in diverse environments to determine Δ TWS at the scale of individual catchments (Barr et al., 2000; Lambert et al., 2013; Marin et al., 2010; Smith et al., 2017). Geological weighing lysimetry has been suggested as suitable for mapping the variability of Δ TWS within the Bengal Basin (Bardsley and Campbell, 2000; Burgess et al., 2017), complementary to basin-scale estimates based on the Gravity and Climate Recovery Experiment (GRACE) satellite mission (Shamsudduha et al., 2012; Tapley et al., 2004; Tiwari et al., 2009).

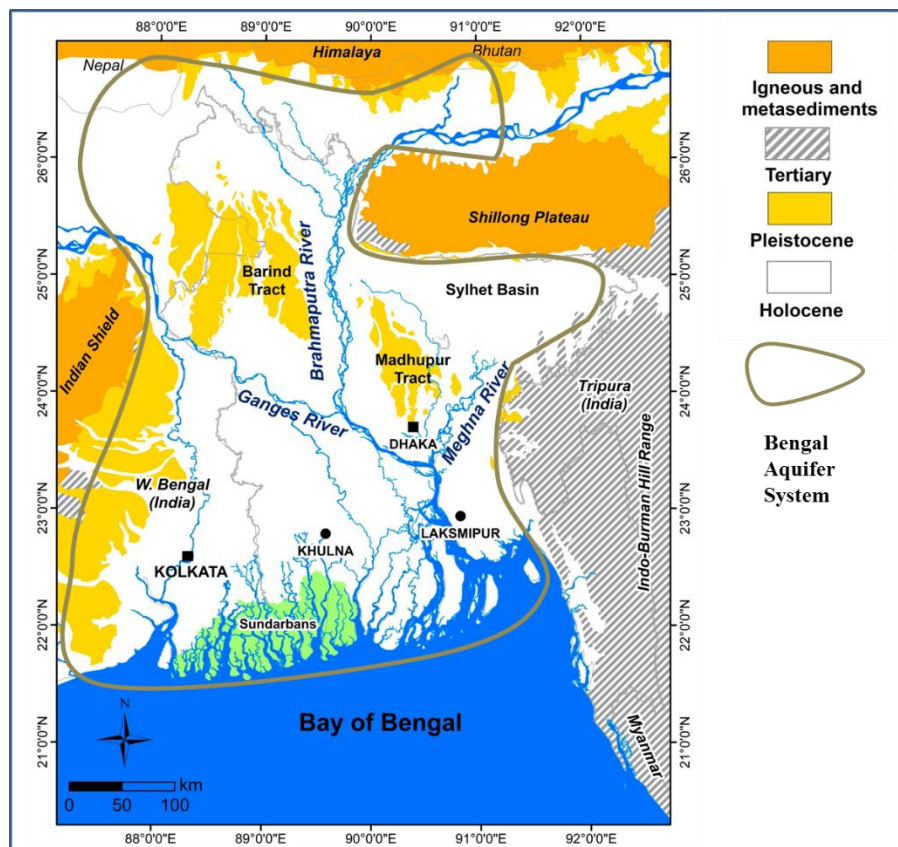
The purpose of this paper is to explore the behaviour of the BAS as a poroelastic aquifer subject to a variety of extensive TWS mechanical and hydraulic loads. For this, we treat separate components of TWS across the GBM floodplains as *inundation* (free-standing surface water such as paddy, floods, beels, and ponds), *unconfined storage* (water in the unsaturated zone and in saturated pores in the intermittently saturated zone of the aquifer), *elastic storage* (water in the saturated pores in the permanently saturated zone), and *rivers* (surface water flowing in rivers and drainage channels). Processes that alter the TWS loads include rainfall and evaporation, rising and falling river stage, flooding and drainage of the land surface, varying soil moisture storage and a fluctuating water table. Groundwater pumping modifies the water balance and induces additional hydro-mechanical responses. These processes differ in their timing, the geometry of the TWS stores they affect and the relationship between their resultant hydraulic and mechanical expressions. First, we apply the concept of *partial* coupling to seek characteristic responses of the aquifer to extensive TWS loads originating as (a) surface water inundation, (b) water table fluctuation and (c) water bodies hydraulically isolated from the aquifer. These loading styles are examined with and without pumping. The results address important questions for the BAS which are likely also relevant to similarly extensive and strategically important fluvio-deltaic aquifer systems elsewhere in south Asia (Benner et al., 2008; Fendorf et al., 2010; Larsen et al., 2008; Tam et al., 2014; Xu et al., 2011): how can piezometer heads in the poroelastic aquifer be used to indicate recharge, as required for conventional groundwater resources management; under what conditions can piezometer heads be used to measure Δ TWS using geological weighing lysimetry; can ground surface deflections be related to changes in groundwater storage; and what errors may arise if the poroelastic behaviour of the aquifer is ignored? Second, we apply the partial coupling approach to these questions in the BAS, with reference to multi-level piezometer data from Khulna and Laksmipur in southern Bangladesh (Fig. 1).

2 Methods

We firstly set out the partially-coupled 1D poromechanical approach that we use to examine the implications of specific surface (upper boundary) loading scenarios, with aquifer parameters set to represent the BAS underlying the GBM floodplains (Fig. 1). We consider an equivalent homogeneous uniform medium, as well as a layered structure based on lithological sections.



96 The results provide a diagnostic framework which we apply to analysis of loading styles at Khulna and Laksmipur in southern
 97 Bangladesh.



98
 99 **Figure 1. Location map showing the extent of the Bengal Aquifer System (BAS) and the Ganges-Brahmaputra-Meghna (GBM)**
 100 **floodplains.**

101



102 2.1 Poromechanical equations

103 We concentrate on the isothermal coupling between water flow and the elastic behaviour of the BAS sediment, and assume
 104 that the aquifer material behaves in a linear-elastic way. This is likely to be reasonable under repeated mechanical load-unload
 105 cycles, provided there is no secular decline in groundwater level sufficient to cause effective stress to exceed the previous
 106 loading maximum.

107 The governing equations for elastic deformation of a porous solid can be derived from the constitutive equations for stress,
 108 force equilibrium and strain compatibility. In 3D, the poro-elastic constitutive relations between elastic stress and strain are
 109 the same as the classical relationships for an elastic solid coupled to the pore-pressure by Terzaghi's effective stress law
 110 (Neuzil, 2003):

$$\sigma_{ij} = 2G\varepsilon_{ij}\delta_{ij} + 2G\frac{\nu}{1-2\nu}\varepsilon_{kk}\delta_{ij} + \alpha_B p\delta_{ij} \quad (1)$$

111 where, δ_{ij} is the Kronecker delta (which is zero when $i \neq j$ and one when $i = j$) and following the Einstein Summation
 112 convention; stresses (σ_{ij}) and strains (ε_{ij}) are positive in compression; p is the porewater pressure (Pa), ν is Poisson's ratio (-
 113), G is the shear modulus (MPa), and $\alpha_B = 1 - K/K_s$, where, K (MPa) is the bulk modulus of the porous medium and K_s
 114 (MPa) is the bulk modulus of the solid grains. Here we assume that the solid grains are effectively incompressible ($K_s \gg K$)
 115 and hence $\alpha_B = 1$.

116 Equation (1) can be simplified to 1D where there is a uniform mechanical load with wide lateral extent such that there are no
 117 lateral strains. The medium is considered to sit on a rigid base, with the top surface free to move, so strain can only be vertical,
 118 thus:

$$\sigma_{zz} = K'\varepsilon_{zz} + \alpha_B p \quad (2)$$

119 where,

$$K' = 3K(1 - \nu)/(1 + \nu) \quad (3)$$

120 and the bulk modulus, K and shear modulus, G are related to Young's modulus E by $K = \frac{E}{3(1-2\nu)}$ and $G = \frac{E}{2(1+\nu)}$. Just as the
 121 elastic equations have a pore pressure term, the isothermal, Darcian groundwater flow equation contains a coupled stress term
 122 (Neuzil, 2003):

$$\nabla \cdot \kappa(\nabla p + \rho g \nabla z) = S_{s3} \frac{\partial p}{\partial t} - S_{s3} \beta \frac{\partial \sigma_t}{\partial t} - gJ \quad (4)$$

123 where κ is the hydraulic conductivity (m s^{-1}), p is the pore pressure (Pa), z is the elevation (m), J is a source term used here
 124 to simulate groundwater abstraction by pumping and $\sigma_t = (\sigma_{xx} + \sigma_{yy} + \sigma_{zz})/3$ (Pa).

125 Changes to σ_t (here termed 'mechanical loads') are applied as a boundary condition at the surface, and are transmitted by the
 126 solid skeleton to the entire solid at the acoustic velocity. This represents partial 'coupling'; if there are no internal loads
 127 applied and provided the changes to the surface load are known, then the flow equation can be solved without a need to solve
 128 the elastic equations. Deformations can be found from Eq. (2), in conjunction with the compatibility relationships.



129 The 3D specific storage is defined as:

$$S_{s3} = \rho g \left[\left(\frac{1}{K} - \frac{1}{K_s} \right) + \left(\frac{n}{K_f} - \frac{n}{K_s} \right) \right] \quad (5)$$

130 where n is the porosity, and K_f is the modulus of the water (MPa). The (3D) loading efficiency, or Skempton's coefficient, β ,
 131 is defined as:

$$\beta = \frac{\left(\frac{1}{K} - \frac{1}{K_s} \right)}{\left(\frac{1}{K} - \frac{1}{K_s} \right) + \left(\frac{n}{K_f} - \frac{n}{K_s} \right)} \quad (6)$$

132 In the event of uniform areal mechanical loading, and where lateral strains are negligible, Eq. (4) simplifies to 1D:

$$\nabla \cdot \frac{k \rho g}{\mu} (\nabla p + \rho g \nabla z) = S_s \frac{\partial p}{\partial t} - S_s \xi \frac{\partial \sigma_{zz}}{\partial t} - gJ \quad (7)$$

133 where $\xi = \beta(1 + \nu)/[3(1 - \nu) - 2\alpha\beta(1 - 2\nu)]$ is the one-dimensional loading efficiency and S_s is the one-dimensional
 134 specific storage (van der Kamp and Gale, 1983)

$$S_s = S_{s3}(1 - \lambda\beta) \quad (8)$$

135 where $\lambda = 2\alpha_B(1 - 2\nu)/3(1 - \nu)$.

136 We therefore consider a simplified system: a 1D column of aquifer with no-flow boundaries on the sides and base, and no
 137 horizontal strain (Fig. 2). On the upper boundary, the changing TWS is simulated by means of a changing head and a changing
 138 mechanical load, according to the nature of the contributing hydrological components. Under this simplification, vertical
 139 displacement at the surface will arise in only two ways: by contraction or expansion of the pore space where there is a net
 140 change in the volume of water in the column, and by contraction or expansion of the pore water. Being limited to 1D movement,
 141 these volume changes are entirely taken up by vertical displacement.

142 The reference frame is the base of the model which is assumed fixed in space and set at 1 km depth, acknowledging the
 143 variation in aquifer thickness between south-east Bangladesh, 3000 m (Michael and Voss, 2009b) and West Bengal, 300 m
 144 (Mukherjee et al., 2007). Within this domain, equations (2) & (7) are solved analytically for a homogeneous uniform material
 145 in the absence of pumping, and numerically where layers of individually homogeneous materials are simulated, with and
 146 without pumping. Where pumping is simulated, the water is assumed to be taken uniformly from the pumping-interval. For
 147 simplicity, earth-tides are neglected.

148 2.2 Analytical solution

149 Taking Eq. (7) and assuming homogeneous K , E and that $J = 0$, converting p to metres head, h (i.e. $h = \rho g p + z$), and σ_t to
 150 metres of load (i.e. $L = \sigma_t / \rho g$, where ρ (kg m^{-3}) is the density of water and g (m s^{-2}) is the acceleration due to gravity)
 151 (Burgess et al., 2017; van der Kamp and Schmidt, 1997) gives:

$$D \frac{\partial^2 h}{\partial z^2} = \frac{\partial h}{\partial t} - \xi \frac{\partial L}{\partial t} \quad (9)$$



152 where 1D hydraulic diffusivity is defined as $D = \frac{k\rho g}{\mu S_y}$.

153 Applying the following sinusoidal hydraulic and mechanical loading boundary conditions to Eq. (9) where we introduce
 154 parameter, α , which can be set to zero to give the case of a load in the absence of a varying head, and otherwise is kept at 1:

$$h(0, t) = H(t) = \alpha H_0 \cos(\omega t) \quad (10)$$

$$L(t) = S_y H_0 \cos(\omega t)$$

155 The following solution is obtained:

$$h(z, t) = \alpha B \cos(\omega t - \psi) \quad (11)$$

156 where ψ is the lag (in radians) behind the head $H(t)$ and mechanical loads $L(t)$ at the boundary and:

$$B = \sqrt{\gamma^2 + 2\gamma(\alpha - \gamma)e^{-\theta} \cos(\theta) + (\alpha - \gamma)^2 e^{-2\theta}} \quad (12)$$

$$\psi = \tan^{-1} \left(\frac{(\alpha - \gamma) \sin(\theta)}{(\alpha - \gamma) \cos(\theta) + \gamma e^{\theta}} \right)$$

$$\theta = z \sqrt{\frac{\omega}{2D}} = z \sqrt{\frac{\pi}{DT}} \quad \text{and} \quad \gamma = S_y \xi$$

157 In the event that the mechanical load, L , is negligible compared to applied head H (e.g. where either S_y is very small
 158 or ξ is very small), the hydraulic-only solution is well known (van der Kamp and Maathuis, 1991):

$$h(z, t) = H_0 \exp(-\psi) \cos(\omega t - \psi) \quad (13)$$

159 where the lag is now $\psi = \theta$. Thus, the lag increases with depth or with increasing forcing frequency and the amplitude
 160 decreases exponentially with θ .

161 Displacement and change in groundwater storage can be calculated as the time integral of velocity at the surface. Applying
 162 Darcy's law at the surface ($z=0$) and integrating gives:

$$u = \Delta S = \int_0^t K \left. \frac{dh}{dz} \right|_{z=0} dt' \quad (14)$$

163 Equation (14) can be computed by differentiating Eq. (11) w.r.t. z and then numerically integrating over time. Alternatively,
 164 the change of storage can be reported from the numerical model.

165 2.3 Numerical solution

166 We used the COMSOL Multiphysics® software, validated against the analytical solutions for uniform permeability, to solve
 167 the stress and flow equations (1) and (4). The finite-element model is unrestricted in terms of spatial distribution of parameter
 168 properties and in terms of the boundary condition functions.

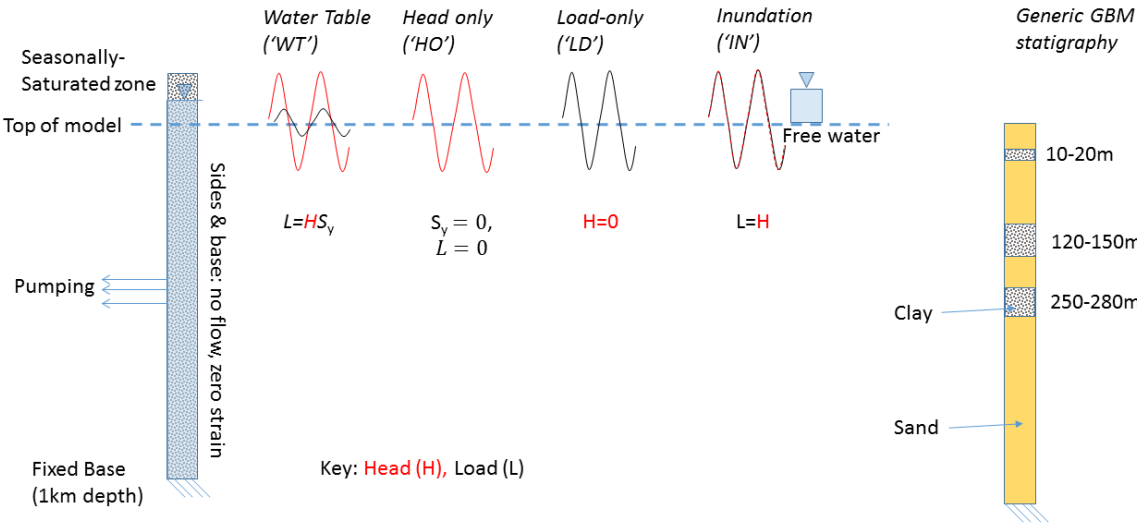


2.4 Parameter allocation

Selected parameter values for the BAS underlying the GBM floodplains are given in Fig. 2. The bulk values for the uniform representations are close to the harmonic average of the series components. We next discuss the context in which these parameter selections are made.

2.4.1 Modulus of elasticity, storativity and loading efficiency

Text-book S_s values (Domenico and Schwartz, 1998) for the materials in the Bengal Basin range between approximately $1 \times 10^{-5} \text{ m}^{-1}$ (dense sandy gravel) and $1 \times 10^{-2} \text{ m}^{-1}$ (plastic clay). In large-scale modelling of head recession data in the basin Michael & Voss (Michael and Voss, 2009a) achieved their best fits when S_s was $9.4 \times 10^{-5} \text{ m}^{-1}$ taking pumped abstraction to be areally uniform. This is the basis for the range in specific storage, S_s , for the BAS (Fig. 2).



178

	Uniform <i>homogeneous</i>	Layered representation						
		1 (sand)	2 (silty-clay)	3 (sand)	4 (silty-clay)	5 (sand)	6 (silty-clay)	7 (sand)
Thickness (m)	1000	10	10	100	30	100	30	720
S_y (-)	0.1 ¹	0.1	-	-	-	-	-	-
S_s (m^{-1})	0.00001 ²	1×10^{-5}	1×10^{-4}	1×10^{-5}	1×10^{-4}	1×10^{-5}	1×10^{-4}	1×10^{-5}
K_v (ms^{-1})	0.00000005 ³	1×10^{-5}	1×10^{-8}	1×10^{-5}	1×10^{-8}	1×10^{-5}	1×10^{-8}	1×10^{-5}



E (MPa)	82.07	850.89	82.07	850.89	82.07	850.89	82.07	850.89
β (-)	0.996	0.961	0.996	0.961	0.996	0.961	0.996	0.961
ξ (-)	0.993	0.932	0.993	0.932	0.993	0.932	0.993	0.932

179
 180 **Figure 2. The 1D model showing (top) the upper surface boundary conditions with head as red lines and mechanical load (weight)**
 181 **as black lines, expressed as metres of water; and a representative stratigraphy for the BAS underlying the GBM floodplains, with**
 182 **the profile depth being 1 km; and (bottom) parameter values for the uniform and layered 1D representations. Porosity is taken as**
 183 **0.1 throughout; $\nu=0.25$; E , β and ξ are calculated using Equations (5) and (6). ¹ Shamsudduha et al., 2011; ² Burgess et al., 2017; ³**
 184 **Michael and Voss, 2009b.**

185
 186 Specific storage S_s and Young's Modulus E are related though Eq. [5] and to the loading efficiency β via Eq. (6). These inter-
 187 relationships are plotted in Fig. 3. It is notable that for $E < 1$ GPa, $\beta > 0.95$ and $S_s > 1 \times 10^{-5} \text{ m}^{-1}$. Thus the loading efficiency only
 188 falls significantly below 1 for materials stiffer than around 1 GPa, and where the specific storage is less than $1 \times 10^{-5} \text{ m}^{-1}$.
 189 Uncemented sediment is thus expected to have $\beta \sim 1$ (Bakker, 2016); on this basis the BAS sediment is unlikely to be
 190 sufficiently stiff in the top few hundred metres to allow decoupling of the stress and flow equations. This is confirmed by in
 191 situ, high-pressure dilatometer measurements (de Silva et al., 2010) giving E within the broad range for sediments given in Fig.
 192 3.

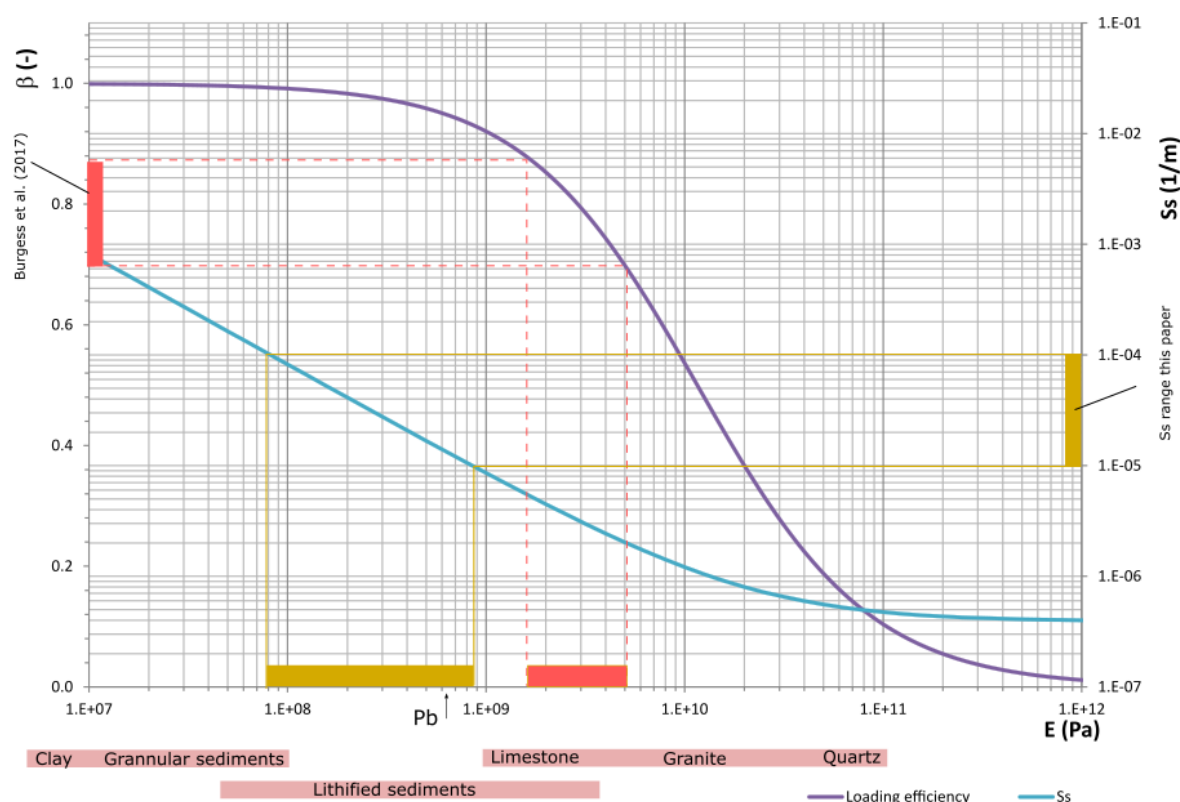


Figure 3. Relationship between 1D Specific storage (S_s), Young's modulus (E) and 3D loading efficiency (β) using equations (5) and (6) assuming porosity of 0.1 and Poisson's ratio of 0.25. Projections show the corresponding inferred ranges of E based on the S_s range applied (1×10^{-5} - $1 \times 10^{-4} \text{ m}^{-1}$) and the loading efficiencies calculated via barometric efficiency estimates (0.69-0.87) by Burgess et al. 2017. Pink bars show indicative ranges for common geological materials. Arrow indicates data from 73 m depth at Padma Bridge (Pb) (De Silva et al., 2010).

Estimates of loading efficiency based (Jacob, 1940) on barometric efficiency are rather lower: a range of 0.69-0.87 has been determined at Laksmipur in the GBM sediment (Burgess et al., 2017). This is potentially indicative of a considerable stiffening due to burial (E in the range 6-17 GPa), indicating S_s in the range 1×10^{-6} to $9 \times 10^{-8} \text{ m}^{-1}$. Such a condition might be expected in a Gibson soil (Gibson, 1974; Powrie, 2014). However, the Laksmipur estimates do not decrease systematically with depth, possibly due to changes in stiffness in different materials. Therefore for the purposes of this paper we adopt S_s estimates based on field measurements and use the corresponding β and E values.

2.4.2 Hydraulic conductivity

Basin scale modelling suggests a horizontal-vertical anisotropy for hydraulic conductivity in the BAS of $\sim 10,000$ (Michael and Voss, 2009a; Ravenscroft et al., 2005). This may be explained as an effective, large-scale value incorporating finer-scale detail of the highly heterogeneous sedimentary record of the past deltaic environment where low permeability lenses and



drapes are laterally discontinuous (Hoque et al., 2017). Michael and Voss (2009b) cite aquifer tests (Hussain and Abdullah, 2001) conducted by the Bangladesh Water Development Board (BWDB) giving a range for hydraulic conductivity (κ) from 3×10^{-5} to 1×10^{-3} m s⁻¹. Accounting for anisotropy, κ_v may therefore locally be in the range $\sim 1 \times 10^{-9}$ to 1×10^{-7} m s⁻¹. The κ_v values of the uniform and layered representations of the BAS underlying the GBM floodplains (Fig. 2) and of silty-clay in layered representations of the Khulna and Laksmipur sites (Sect. 4) lie within this range.

2.4.3 Specific yield

Specific yield is the drainable porosity of the material in which the water table moves. Michael and Voss (2009a) cite a range from 0.02 to 0.19 in Bangladesh, noting that much of the Basin has a specific yield in the range of 0.02–0.05. We take $S_y=0.1$ and 0.01 as order-of-magnitude values typical for sand and clay respectively (Domenico and Schwartz, 1998).

2.5 Upper boundary conditions and groundwater abstraction

Changes to the shallow water budget which have the potential to be laterally-extensive and uniform include: water arriving as rainfall at the surface and either ponding or moving to the shallow water table as recharge; and water departing the surface or the water table by evaporation, or as runoff to the extensive network of drainage channels. Pumping for domestic and irrigation supply may potentially be considered as areally-uniform, where sufficiently common and over a wide area (Michael and Voss, 2008).

The changing shallow water budget causes a change in mechanical loading to the aquifer system, and if in direct hydraulic continuity with the saturated water column it also causes a change in head. If the shallow water is not hydraulically connected to the saturated aquifer system, the effects of the changing water budget are transmitted to depth by mechanical compression/extension of the sediment, but not by hydraulic diffusion.

Changes to the barometric pressure also apply a laterally-extensive changing force to the surface of the aquifer and to the water column, and earth tides are also laterally-extensive. Both effects are neglected for simplicity here.

To explore the consequences of these hydraulic and mechanical loading sources, the groundwater dynamics associated with three upper surface boundary conditions are modelled here (Fig. 2).

Firstly, the effect of a changing level of free water is examined, such as would be seen in paddy-fields, ponds or during floodwater inundation. This condition is here termed ‘IN’. The change in free-water level is equal to both the change in head and the change in mechanical load at the upper surface (load is here parameterised in metres of water rather than as a stress).

Secondly, the effect of changes to unconfined storage due to a moving water table is examined. This condition is here termed ‘WT’. The change in load is the specific yield times the head. For very small specific yields this condition approaches the hydraulic-only (‘HO’) loading case, whereby there is insignificant mechanical load, despite the change in head.

Thirdly, we examine the effect of a changing surface water store (which could be either free water held above an impermeable barrier, or a perched phreatic aquifer) which is hydraulically isolated from the main aquifer system. A mechanical load only is applied, therefore no head change is applied to the aquifer and this condition is termed ‘LD’.



241 These three TWS loading scenarios are applied in turn to a uniform and a layered representation of the BAS underlying the
242 GBM floodplains. The loading is applied as sinusoidal functions with unit amplitude and time period of 1 year to simulate the
243 annual hydrological cycle.

244 Additionally, the effects of groundwater abstraction are simulated. Abstraction is taken evenly from the depth interval 50-
245 100 m at an average rate of 0.2 m a^{-1} , either as continuous pumping or as discontinuous pumping π out of phase with the TWS
246 load, as a coarse representation of seasonally-varying pumping for irrigation during the dry season.

247

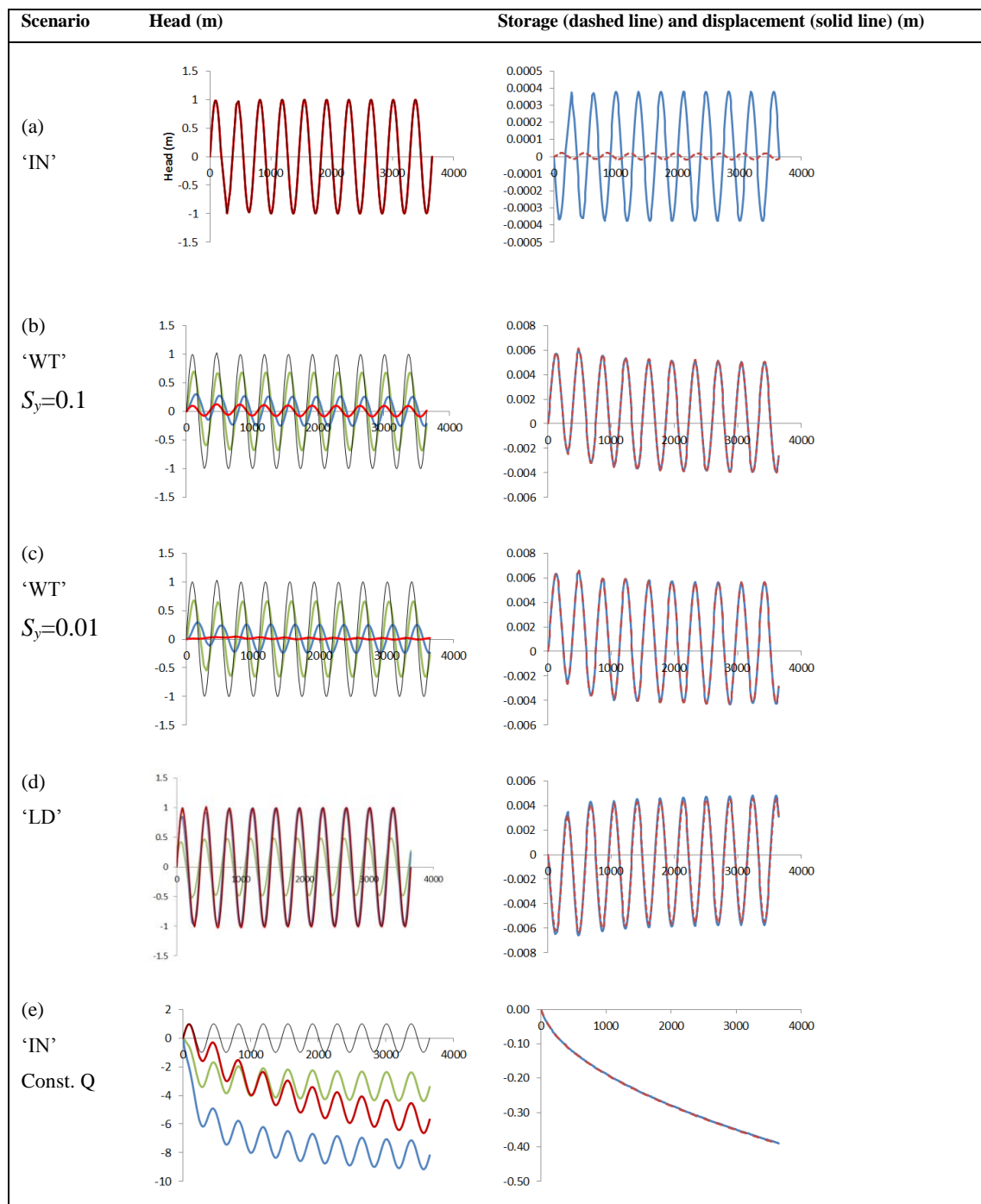
248 3 Forward modelling results

249 The modelled responses of groundwater head to sinusoidal hydraulic and mechanical source terms, together with changes in
250 groundwater storage and ground surface vertical displacements, are illustrated for the GBM environment with uniform
251 properties in Figures 4 and 5. Figure 4 shows the modelled responses over ten years at depths of 30, 100 and 300 m,
252 approximating typical BWDB multi-level piezometers (BWDB, 2013). The depth variations of amplitude and phase for
253 groundwater head and the phase-lag for surface displacement are summarised in Fig. 5. The effect of layering (Supporting
254 Information) is to cause departure from the uniform cases, so interpretation of data in a real, heterogeneous aquifer should take
255 into account local deviation from idealised uniform conditions. However, in general, the loading style ('IN', 'WT', 'LD') and
256 pumping regime are of more significance for the head responses and surface displacements than the detail of the BAS
257 stratigraphy.

258 3.1 The free surface water inundation scenario ('IN')

259 Under free-surface water inundation, head changes are characteristically equal in amplitude at all depths and in-phase with the
260 inundation signal. Away from the top boundary, the instantaneous head due to loading in this case is $h = \xi L$. Since ξ is close
261 to 1 and $H = L$, the head is everywhere almost equal to the mechanical load given that at the top boundary the head is also
262 $h = H$. Therefore under free-surface water inundation in the absence of pumping, piezometers at all depths can be expected to
263 record the surface water mechanical load, effectively operating as weighing lysimeters. The vertical displacement of the ground
264 surface is extremely small (amplitude $\sim 0.4 \text{ mm}$), being due to the small compression of porewater itself over the 1 km
265 simulated depth, and is out of phase with the load (i.e. the ground surface moves downwards under an increasing load). The
266 amplitude of change in saturated storage is infinitesimal ($\sim 0.02 \text{ mm}$). The system is essentially 'un-drained'; water does not
267 flow in or out of the pores which therefore experience only minimal strain.

268



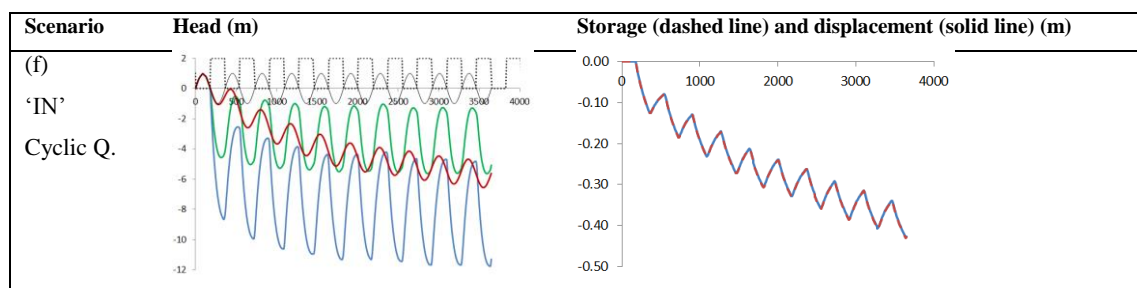


Figure 4. 1D model simulations for the GBM environment, showing results for the scenarios (a) ‘LD’, (b) ‘WT’ ($S_y=0.1$), (c) ‘WT’ ($S_y=0.01$), (d) ‘LD’, (e) ‘IN’ with constant pumping, (f) ‘IN’ with cyclic pumping, (see text for explanation). The x-axis is time in days, shown to 10 years (i.e. 3650 days). The amplitudes reported in the text are calculated from the max-min of the last annual cycle. Left: The y-axis is head, in metres (m). The surface head and/or mechanical load boundary conditions (black line) are expressed as equivalent m head (for the WT condition the unit variation of head is given and the S_y variation in mechanical load is not shown); results are in green (30 m depth), blue (100 m depth) and red (300 m depth) in all cases. For (a) results are co-linear at all depths; for (f) the intermittent pumping is shown as off/on by the square-wave dotted line. Right: The y-axis has dimension of length, in metres (m), showing changes in storage (dashed red line) and surface displacement (solid blue line) for each scenario.

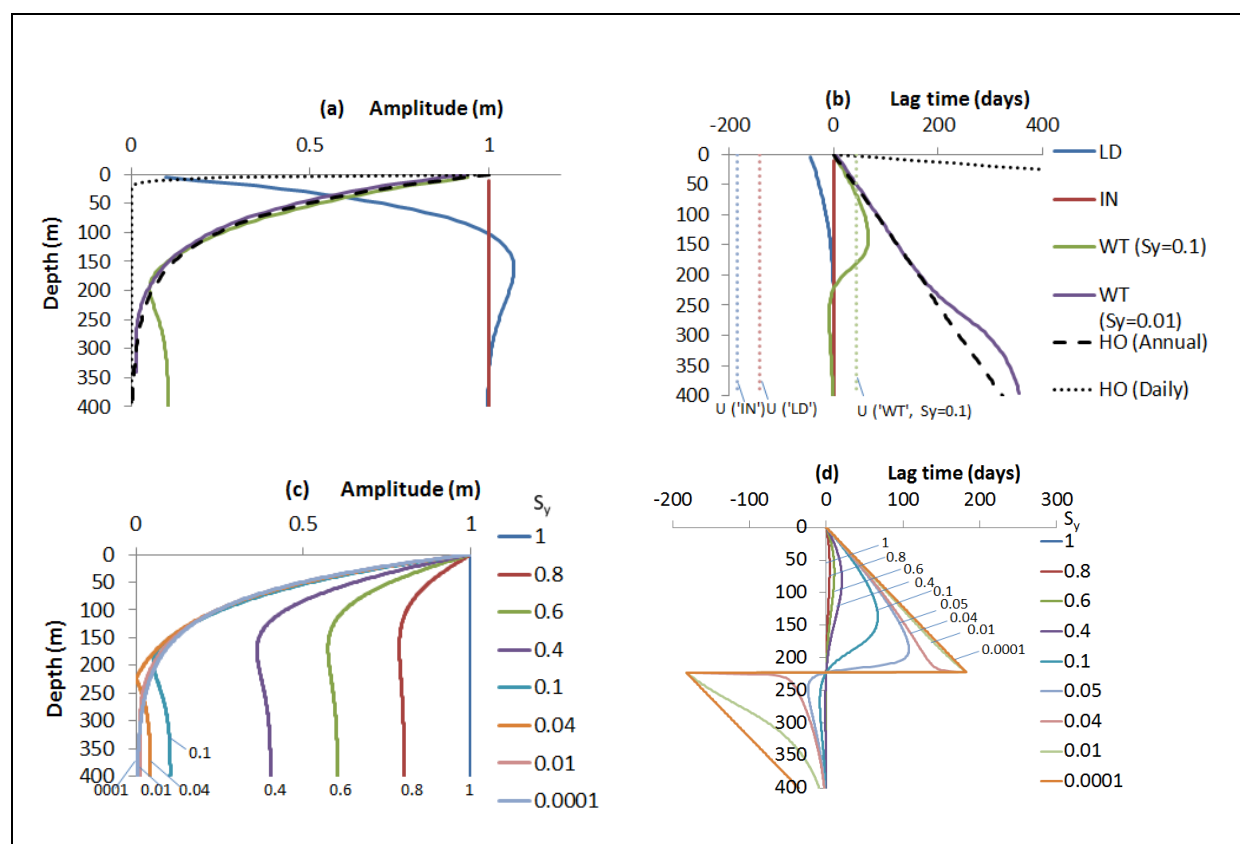


Figure 5. Profiles with depth for (a) amplitude of head response, (b) phase of head response and surface displacement (U), (c) sensitivity of amplitude to S_y for the ‘WT’ boundary condition, (d) sensitivity of phase to S_y for the ‘WT’ boundary condition. For (a) and (b) the colour code for the scenarios ‘LD’, ‘IN’, ‘WT’ ($S_y=0.1$), ‘WT’ ($S_y=0.01$), and HO, is shown in the top right panel (see text for explanation); in (b), displacement for the WT, $S_y=0.01$ scenario overlies that for the WT, $S_y=0.1$ scenario, so is not shown.



3.2 The variable water table scenario ('WT')

By contrast with the 'IN' scenario, head changes determined by a moving water table are depth-variable in amplitude and phase. When $S_y \rightarrow 0$ the 'WT' condition tends to the head-only end-member ('HO') and when $S_y \rightarrow 1$ the 'WT' condition tends to the 'IN' scenario. The maximum lag for $S_y = 0.1$ is at 137 m depth (or $\theta = 1.94$), beyond which it reduces (Fig. 5b). The sensitivity in head to S_y for the 'WT' scenario is illustrated in Fig. 5c. The amplitude of head responses is less than the water table fluctuation at all depths. Moreover, only a deep piezometer such as the one indicated at 300 m (Fig. 4b) will behave as a weighing lysimeter in this scenario. Here, heads are in phase with the water table and have approximate magnitude, $h = \xi L = \xi S_y H$, as in the study by van der Kamp and Maathuis (1991) of a thick aquitard overlying a confined aquifer. At 100 m the amplitude of head change is greater than at 300 m, and lags behind the water table. At 30 m the amplitude of head change is greatest and the lag is less than at 100 m. The difference in the head responses compared to the 'IN' scenario is due to the difference in magnitudes of the applied head and applied load under the 'WT' scenario, causing an instantaneous internal head gradient which subsequently diffuses. Ground surface displacement is ~ 4 mm and lags the load by 44 days. With increased head at the top boundary, the upper surface moves upwards because as higher heads penetrate the aquifer the effective stress is reduced. The lag is due to the time taken for the surface head to diffuse downwards.

3.3 The hydraulically disconnected load scenario ('LD')

Heads in the case of a surface load hydraulically isolated from the aquifer show a third characteristic behaviour. In this case the amplitude of head change increases from zero at the top boundary (Fig. 5a), and counter-intuitively reaches a peak which is greater than the load, 1.07 m at 162 m (or $\theta = 2.29$). The amplitude thereafter tends to ξL at greater depth, whilst the lag tends to zero. Therefore heads in relatively deep piezometers potentially represent the surface load under a 'LD' boundary condition, as in Fig. 4d where the heads at 300 m match the surface load, whereas at 30 m they do not. This is due to upward head diffusion towards the surface where the head boundary condition is $h=0$. The lag which occurs in the 'WT' scenario due to the applied head exceeding the mechanical load is reversed in this 'LD' scenario, becoming a lead time as the applied load exceeds the applied head. Surface displacement is out of phase with the load, leading by $\sim \pi$ radians. The ground surface displacement amplitude of ~ 4 mm is ten times greater than for the 'IN' scenario but is still very small in comparison to the annual variability of order 10 cm measured by GPS (Steckler et al., 2010).

3.4 The influence of pumping

Introduction of pumping from the depth interval 50-100 m causes hydraulic dis-equilibrium which continues well beyond the ten years' simulation, as the head drawdown propagates deep into the profile. As well as drawing water from storage at depth, pumping induces recharge from the surface, there being a downward hydraulic gradient from the surface to the pumped horizon, and upwards from the deeper levels to the pumped horizon. Variable perturbation due to the 'IN' surface load is nevertheless clearly evident in the deep groundwater head measurements following correction for secular decline (Fig. 4e).



313 Elastic displacement, manifested as ground surface decline, exceeds 40 cm after ten years of pumping but, as in the un-pumped
 314 'IN' scenario, the annual fluctuation due to surface loading is vanishingly small (0.03 mm). Thus, in addition to the possibility
 315 of irreversible plastic deformation, elastic strain may gradually increase due to continuous pumping as stored water is drawn
 316 from increasing depths.

317 Intermittent pumping strongly increases the seasonal variation in heads at the depth of pumping and this disturbance diffuses
 318 to adjacent levels. However, as in the case of continuous pumping, the surface load signal is largely preserved in the deep
 319 groundwater head response at 300 m. Also, intermittent pumping induces the same average long-term secular decline in stored
 320 water volume and ground surface displacement as continuous pumping, but with additional annual fluctuation caused by the
 321 pump switching on and off (decline/drawdown during the dry period when the pumps are used for irrigation and recovery
 322 during the rainy season when the pumps are off).

323 3.5 Model results for ground surface displacement

324 Taking into account a small correction for the compressibility of water, surface displacement in the model is almost equal to
 325 the total change in elastic storage in the permanently saturated aquifer. For the cases where pumping dominates the removal
 326 of water, surface displacement is in phase with the pumping (Fig. 4f). For the cases which set up a diffusion of the hydraulic
 327 signal between the surface boundary and the aquifer, the phase of surface displacement depends on the hydraulic (non-loading)
 328 head changes at all depths (Fig. 4b,c,d). Therefore the lag for vertical displacements under the 'LD' surface condition is $\sim\pi$
 329 out of phase with displacement under the 'WT' condition. Note from Eq. [12] that the amplitude and lag are both a function
 330 of $\theta = z \sqrt{\frac{\omega}{2D}} = z \sqrt{\frac{\pi}{DT}}$ and therefore the solutions given here would be scaled in z by any changes to bulk diffusivity, D , and
 331 signal frequency (or time period, T): higher frequency would give the same distribution but for a smaller z and the reverse
 332 would be true for diffusivity. Intermittent pumping produces the largest cyclic displacements, however, in the order of
 333 centimetres, because this condition causes the greatest volume of seasonal drainage from the formation itself. Where there is
 334 non-uniform loading, as produced for example by a variable river stage, lateral groundwater drainage may occur and surface
 335 vertical displacements may be greater under these conditions too.

337 4 Applying the partial coupling analysis to field data

338 Applying the 1D partial-coupling analysis to field data, we examine poromechanical perturbations at two sites, Khulna and
 339 Laksmipur and in southern Bangladesh (Fig. 1). Hourly measurements of groundwater pressure made between April 2013 and
 340 June 2014 in three closely-spaced piezometers between 60 and 275 m depth at each site are illustrated as hydrographs of
 341 equivalent freshwater head in Supporting Information. The objective here is to apply the principles and assumptions of the
 342 partially-coupled hydro-mechanical approach to reproduce the characteristic features of the multi-level groundwater



hydrographs using broadly representative aquifer parameters, rather than to attempt an exact match by inverse modelling. Inspection of the hydrographs at both sites indicates, by reference to Figures 4 and 5, that mechanical loading significantly influences the measured heads. Additionally, the presence of thick clay aquitards at both sites (Figures 6, 7) suggests conditions under which heads may be determined solely by mechanical loads and piezometers might behave as geological weighing lysimeters; a possibility which we put to the test.

The approach at each site is as follows:

- i. A two-component sand-clay stratigraphy is based on site data, and parameter values are selected from the ranges described in Section 2.
- ii. The piezometric readings are compared to examine possible pumping influences which need to be taken into account in the model by means of a simple abstraction pattern. Based on what is known about nearby abstractions an appropriate pumping depth interval is determined. The magnitude of the extraction rate is manually adjusted as a fitting parameter.
- iii. Where a piezometer is uninfluenced by pumping we test its behaviour as a geological weighing lysimeter. The heads in the chosen piezometer are assumed to define the mechanical load at the surface, and this assumption is tested for self-consistency by comparison of the simulations to the data from all three piezometers.
- iv. The nature of the upper head boundary is then examined by reference to the implications for a variety of hydraulic loading conditions. For a ‘WT’ boundary, changing S_y manually as a fitting parameter adjusts the magnitude of the applied heads concomitant with the mechanical load.

4.1 Groundwater levels at Khulna, south-west Bangladesh

At Khulna town (Burgess et al., 2014) piezometers KhPZ60, KhPZ164 and KhPZ271 (the numbers indicate depth to the piezometer screen in metres) are located 700 m from the ~300 m wide tidal Rupsa River, in a grassy compound which also contains municipal water-supply pumping boreholes (Supporting Information). The lithological sequence (Fig. 6) comprises a surface clay layer overlying sand in which KhPZ60 is screened, and a deeper layer of clay at 100 m separating the shallow sand from a deeper sand formation in which KhPZ164 and KhPZ271 are screened. Year-round pumping from 250-300 m depth maintains a consistent downward head difference of ~3 m between the uppermost and the lower two piezometers. It is the transient head variations rather than the absolute steady-state head differences that are of interest here. Bodies of standing water in the vicinity, water in the unsaturated zone, and shallow groundwater combine with the sinuous Rupsa River as sources of TWS load; groundwater pumping is an additional source of hydraulic variation.

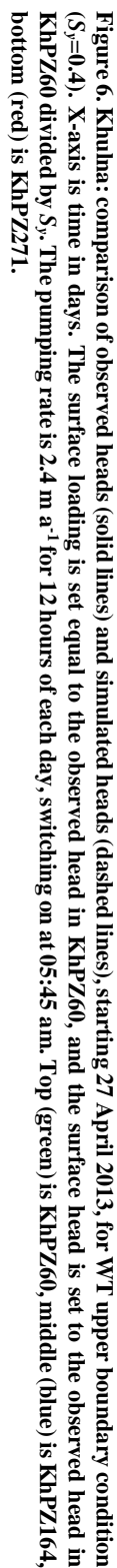
The three Khulna hydrographs are characterised by periodic variations containing tidal frequency components throughout the rising and falling limb of the annual cycle, and a series of episodic increments superimposed on the rising limb during the monsoon season; the annual amplitude of groundwater head variation is ~2.5 m. Amplitude of the tidal frequency components increases between 60 m and 164 to 271 m depth, with no phase lag and with a consistent synchronicity between the piezometer heads and the Rupsa River water level fluctuations including the semi-diurnal and spring-neap cycles (Fig. 6 and Supporting Information). Episodic deflections on the hydrograph rising limbs, coincident with rainfall events, are likewise simultaneous



376 at all measurement depths (Burgess et al., 2014). Therefore by reference to the partial coupling analysis (Figures 4 and 5) It is
 377 evident that heads in the Khulna piezometers respond primarily to mechanical loading by a combination of monsoon water
 378 and tidal loading.

379 At a daily level the time series of groundwater heads in KhPZ164 and KhPZ271 include an additional frequency component
 380 which simple analysis of head differences confirms as the hydraulic influence of the daily municipal pumping schedule from
 381 which KhPZ60 is protected by an intermediate clay layer. Therefore KhPZ60 alone is taken as recording a solely mechanical
 382 loading response and the KhPZ60 head record is applied as the upper boundary condition to represent the varying TWS load
 383 at the surface in a 1D hydro-mechanical model of the Khulna site (Fig. 6), assuming $\beta=1$. The upper boundary resolves all
 384 sources of load acting at the site including from the Rupsa River, which is a linear rather than an areally-extensive load. The
 385 ratio of daily variability in head at KhPZ60 and in the Rupsa River level is ~ 0.06 , therefore the 1.23 m annual variation in river
 386 stage would explain ~ 0.07 m head variation in KhPZ60, only 3% of the total. Therefore 97% of the annual variation in head
 387 at KhPZ60 is attributable to changes in TWS other than load transmitted from the river, representing areally-extensive loads
 388 as required by the 1D partially-coupled analysis. Given the relatively well-drained urban context at Khulna and the absence of
 389 areally-extensive open water that otherwise characterises the rural areas of the GBM floodplains, a ‘WT’ condition is most
 390 likely the dominant loading style, but other sources of loading may also contribute. The layered structure of the Khulna model
 391 (Fig. 6) has clay at 0-50 m and 100-150 m with sand in between. The daily municipal pumping cycle is implemented as a
 392 source term of 2.4 m a^{-1} for 12 hours of each day applied over the interval 200 to 350 m, the rate having been manually adjusted
 393 by reference to the daily head fluctuations in KhPZ164 and KhPZ271.

394
 395
 396
 397
 398
 399
 400
 401
 402
 403
 404
 405
 406
 407
 408
 409





410

411 Figure 6 compares the measured groundwater heads with the heads simulated by the model under the assumption of a ‘WT’
 412 boundary with S_y assigned a value of 0.4, with $\kappa_{sand} = 1 \times 10^{-5} \text{ m s}^{-1}$, $\kappa_{clay} = 1 \times 10^{-9} \text{ m s}^{-1}$, $S_s = 10^{-4} \text{ m}^{-1}$ (corresponding to
 413 $E = 82.07 \text{ MPa}$), $\nu = 0.25$ and $n = 0.1$. The results are insensitive to S_y being varied in the range from 0.1 to 1 (the latter being
 414 equivalent to an ‘IN’ boundary), and are near-identical in the case of a ‘LD’ boundary (Supporting Information). This is
 415 because the upper clay effectively isolates the piezometers from the surface hydraulically.

416 4.2 Groundwater levels at Laksmipur, south-west Bangladesh

417 At Laksmipur (Burgess et al., 2017) the piezometers LkPZ91, LkPZ152 and LkPZ244 are situated in a rural region of rice-
 418 paddy and tree plantations on the Lower Meghna floodplain (Supporting Information), 10 km distant from the River Meghna
 419 and 8 km from municipal boreholes which pump from 270–300 m depth. Seasonal pumping from depths up to 100 m for rice
 420 irrigation is common in the vicinity. The lithological sequence indicates fine sand with occasional silty clay layers. The
 421 hydrographs are characterised by a sequence of episodic increments in groundwater head associated with periods of heavy
 422 rainfall producing a rising limb of amplitude $\sim 1 \text{ m}$ through the monsoon season; during the dry-season recession, minor
 423 periodic fluctuations of order 0.01 m containing atmospheric frequency components become more clearly evident (Burgess et
 424 al., 2017). The episodic increments are almost synchronous and of consistent magnitude at all piezometer depths, indicative
 425 by reference to Figures 4 and 5 of groundwater heads responding dominantly to mechanical loading and unloading due to
 426 changes in TWS above the aquifer surface.

427 Here, cyclical head differences between LkPZ244 and the shallower two piezometers indicate hydraulic influences of dry-
 428 season pumping on the LkPZ91 and LkPZ152 hydrographs, whereas downward propagation of the hydraulic signals to
 429 LkPZ244 is prevented by the clay layer between 170 and 200 m depth. Therefore LkPZ244 is taken as recording a solely
 430 mechanical loading response and the LkPZ244 head record is applied as the upper boundary condition to represent the varying
 431 TWS load at the surface in a 1D hydro-mechanical model of the Laksmipur site (Fig. 7). All styles of upper boundary were
 432 applied (‘IN’, ‘LD’, and ‘WT’ with a range of S_y values, see Supporting Information D) in an attempt to distinguish the
 433 dominant source of TWS load around the site from the boundary style leading to the best fit with piezometer measurements.
 434 In all other respects the models incorporate the dimensions and assumptions as described in Sect. 3, with sand ($\kappa_{sand} = 1 \times 10^{-5} \text{ m s}^{-1}$) and three clay layers (BWDB, 2013) at 25–30 m, 115–130 m and 170–200 m ($\kappa_{clay} = 1 \times 10^{-8} \text{ m s}^{-1}$), and $E = 82.07 \text{ MPa}$.
 435 A simple dry-season pumping regime over a 105 day period starting 17 November 2013 is implemented as a source term of
 436 0.04 m a^{-1} applied over the interval 30 to 70 m in the model, manually adjusted by reference to the LkPZ91 and LkPZ152
 437 hydrographs.
 438

439

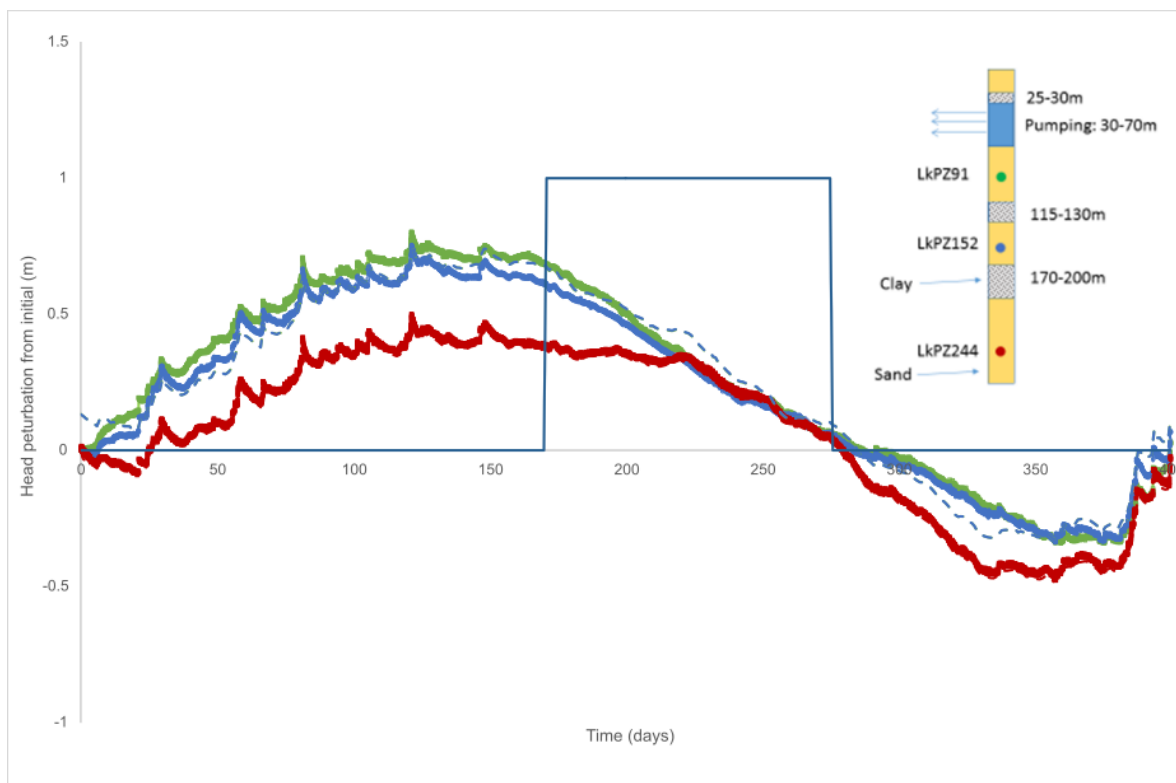


Figure 7. Laksmipur: comparison of observed heads (solid lines) and simulated heads (dashed lines) starting 31 May 2013, for ‘WT’ upper boundary condition ($S_y=0.8$), for LkPZ91 (green), LkPZ152 (blue) and LkPZ244 (red). X axis is time in days. The surface loading is set equal to the observed head in LkPZ244, and the surface head is set to the observed head in LkPZ244 divided by S_y . The pumping rate is 0.04 m a^{-1} for the period shown (1 for ‘on’, 0 for ‘off’).

For LkPZ244 the simulated heads are an excellent match with measurements over the entire period. The simulated heads for the shallower two piezometers LkPZ91 and LkPZ152 most closely match the measurements under a ‘WT’ boundary with S_y assigned a value of 0.8 (Fig. 7 and Supplementary Information). The consistently higher simulated heads compared to observations at LkPZ152 could be simply explained by the sands at that depth having a lower loading efficiency. The model results therefore confirm that LkPZ244 is isolated from the hydraulic effects of water table variation and of seasonal pumping, and the LkPZ244 groundwater head variation over the observation period is determined solely by mechanical loads at the surface. Therefore LkPZ244 is validated as acting effectively as a geological weighing lysimeter (Burgess et al., 2017).

For the shallower piezometers, the best fit value for S_y is higher than is reasonable for fine sand and more likely indicates the combined effects of a variable water table and fluctuating levels of standing water, in drainage channels and on paddy fields around the piezometer site, consistent with the field situation. As a consequence of seasonal pumping at 0.04 m a^{-1} , the model shows groundwater is both drawn from storage and induced as recharge from the upper surface, but the amplitude of saturated



storage fluctuation is only 6 mm, therefore changes to the water budget are dominated by recharge to the water-table. The surface displacement is predicted at 6 mm amplitude, in phase with the changes in storage.

5 Discussion

5.1 Aquifer responses to discrete modes of terrestrial water variation

Models based on the 1D partially-coupled hydro-mechanical analysis confirm that substantial poroelastic influences should be expected in the Bengal Aquifer System, and that groundwater heads respond characteristically to changes in specific terrestrial water stores (Figures 4 and 5). Only laterally-extensive flooding above an aquifer fully saturated to the ground surface (the ‘IN’ loading style) will drive instantaneous and synchronous head variations at all depths determined by the loading efficiency, inducing negligible flow of groundwater. In any situation involving a variable water table (the ‘WT’ loading style) and for any variable loads hydraulically disconnected from the aquifer (the ‘LD’ style), hydraulic gradients are imposed due to the unequal magnitude of stress and head at the surface. These gradients take time to dissipate, depending on the frequency of the signal fluctuation and the aquifer hydraulic diffusivity, and so lead to differences in amplitude and phase of the head response with depth. In these situations, the relative importance of the hydraulic and mechanical influence is controlled by the aquifer hydraulic diffusivity, the loading efficiency and the depth of interest. In the case of a fluctuating water table, the difference between the head and stress signals is a function of the specific yield, S_y , in the zone of fluctuation.

The characteristic responses of the aquifer might therefore provide a key to identifying the terrestrial water store dominating Δ TWS, by monitoring vertical profiles of groundwater head. Multiple terrestrial water stores will normally contribute, however, as at Laksmipur and Khulna, so a unique identification may not be possible. This limitation is inherent to the 1D analysis, which resolves all the contributions to load into one upper boundary condition respectively for head and stress. The analysis indicates how different loads and dynamic responses superpose to produce the observed groundwater hydrographs. In principle, key aspects of the water balance may be better estimated by de-convolving known components of the Δ TWS signal. At Khulna and Laksmipur, the 1D partially-coupled analysis leads to good agreement between simulated and observed heads consistent with the local conditions, confirming it as a suitable basis for representing the poroelastic behaviour of the BAS.

5.2 Significance for groundwater monitoring and geological weighing lysimetry

In terms of the extent to which piezometer water levels indicate recharge and drainage, it is only where there is a rapid hydraulic connection between the piezometer and the water table that the piezometer will be sensitive to head change at the water table and therefore to changes in unconfined storage. If a piezometer is hydraulically isolated from surface water and/or the water table and is beyond other transient hydraulic influences, it can respond to changes in the weight of the TWS load, acting as a geological weighing lysimeter (Smith et al., 2017; van der Kamp and Maathuis, 1991). In this case, where the changing load is due to a moving water table, knowledge of the loading efficiency allows the load measurement to be converted into an estimate of recharge and discharge.



In all other situations, a wide range of coupled hydro-mechanical responses can be expected, as we have shown for the BAS (Figures 4 and 5). Seasonally-variable groundwater heads (Fig. 4) are therefore open to misinterpretation as seasonally-variable groundwater storage, leading to error in determination of recharge if the poroelastic nature of the response is neglected. Consider heads at 30 m, a common depth for Bangladesh Water Development Board (BWDB) monitoring boreholes (Shamsudduha et al., 2011). For the case of a variable load hydraulically disconnected from the aquifer (Fig. 4d) the annual water level rise is equal to half the amplitude of the load yet augmentation of elastic storage, by definition in this case, is nil. For the case of variable TWS inundation (Fig. 4a) the annual groundwater level rise is equivalent to the annual depth of inundation yet augmentation of elastic and unconfined storage is insignificant. Conversely, relative to a variable water table (Fig. 4b,c) groundwater fluctuation at 30 m depth is attenuated. Failure to account for this would lead to an underestimate of recharge to unconfined storage by about 30%. The error increases as hydraulic diffusivity decreases, therefore errors could be expected to be greater in the coastal regions of the Bengal Basin where the thickness of silty-clays is greater (Mukherjee et al., 2007). Considerable caution is therefore necessary in the use of even relatively shallow piezometers as indicators of recharge to the water table. A true indication of recharge requires either a shallow tubewell screened over the depth interval of actual water table fluctuation, or a deep piezometer responding as a geological weighing lysimeter to the varying mass provided by a fluctuating water table. In the latter case it is recharge to the shallow water table that is measured, not recharge at the depth of the piezometer.

The 1D hydro-mechanical framework can be applied as a test for the special cases where groundwater head responds solely to mechanical load, and hence to validate the use of geological weighing lysimetry. The laterally-extensive loading criterion inherent to the 1D analysis must apply, and the piezometer screen must be isolated or distant from hydraulic transients originating at the surface or from pumping. We have shown for the BAS that these requirements most likely occur at depths beyond about 250 m, as in the case of ‘WT’ and ‘LD’ loading styles in the absence of pumping (Fig. 5). The inundation (‘IN’) style of TWS variation leads to instantaneous transmission of head without loss of amplitude at all depths; in this case piezometers at all depths provide a mechanical record of Δ TWS rather than a hydraulic record of storage variation and to infer recharge would lead to 100% error. Our analysis demonstrates a solely mechanical loading response at 244 m depth at Laksmipur, below the level of seasonal irrigation pumping, and at 60 m depth at Khulna, above the level of deep pumping for municipal water supply.

5.3 Significance for ground surface displacements and groundwater storage changes

The models also demonstrate the amplitude and phase of ground surface displacement as a hydro-mechanical consequence of varying terrestrial water stores, and the significance of pumping (Fig. 4e and 4f). Under simplifications associated with the 1D model, vertical surface displacements relative to a fixed model base at 1 km depth are approximately equal to the change in elastic storage, the small difference being due to compressibility of water. These changes are minor in the BAS under all TWS loading styles, in the order of mm, compared to the displacements in the case of seasonal groundwater pumping which are in the order of cm. Seasonal surface displacements in the order of cm have



also been attributed to strain acting over a depth scale of hundreds of kilometres due to the load applied by monsoonal inundation over the entire Bengal Basin (Steckler et al., 2010). Strains due to seasonal groundwater pumping at shallow depths may therefore be in the same order of magnitude but out of phase with crustal strain, making ground surface deflections a poor proxy for changing elastic storage in the aquifer. As a corollary, interpretation of seasonal ground surface fluctuations across the GBM floodplains solely in terms of deep crustal deformation (Steckler et al., 2010) potentially requires reassessment in the light of BAS aquifer poroelasticity.

5.4 Limitations and further consequences

In our analysis we have based values for the 3D loading efficiency, β (0.961-0.996) and Young's Modulus, E (82-851 MPa) in the BAS on field measurements of S_s , for the sake of internal hydro-mechanical consistency, but we have noted a discrepancy with lower values for the 1D loading efficiency ξ (0.69-0.87) derived from determinations of barometric efficiency (Burgess et al., 2017). These differences require attention, but the overall conclusions on the significance of poroelastic behaviour in the BAS and the pattern of poroelastic responses characteristic of specific upper surface TWS boundary conditions are unaffected.

Under certain circumstances the extensive load assumption inherent in the 1D analysis may break down. Rivers, as linear sources of head and load, can be accommodated within the 1D framework where their contribution to the TWS load is minor as demonstrated at Khulna. In general however, rivers should be expected to impose laterally variable heads and require a more generalised 2D or 3D fully-coupled poro-mechanical treatment (Boutt, 2010; Pacheco and Fallico, 2015). An equivalent constraint applies to strains, an additional reason for surface displacement not to offer a secure proxy for groundwater storage in the BAS. The dense distribution of rivers, distributaries and drainage channels in the Bengal Basin makes the BAS widely vulnerable to loading effects that may not adequately be reduced to a 1D description; 13% and 47% of 1035 piezometers in the BWDB groundwater monitoring network lie within 1 and 5 km respectively of a river.

6 Conclusions

We argue that a 1D *partially-coupled* approach to hydro-mechanical processes, whereby the loading term is included in the flow equation without the need to simultaneously compute the elastic equation, is a suitable basis for representing the poroelastic behaviour of the Bengal Aquifer System when surface conditions can be treated as areally-extensive. Applying a 1D *partially-coupled* hydro-mechanical analysis we have shown how the BAS responds characteristically to specific sources of terrestrial water storage variation. Rivers can be incorporated as a component of the 1D load where their contribution is small, but in general will require a 2D or fully 3D treatment.

Groundwater levels, groundwater recharge, vertical groundwater flow and ground surface elevations are all influenced by the poroelastic behaviour of the BAS. Our results expose the error of the conventional assumption of de-coupled hydraulic behaviour which underlies previous assessments of recharge to the BAS. Also they demonstrate the complexities in applying



ground surface displacements as a proxy measure for variations in groundwater storage. We propose that the 1D *partially-*
coupled analysis can be applied to validate when geological weighing lysimetry is applicable in the BAS. In some situations,
 geological weighing lysimetry offers an alternative approach to recharge assessment.

Author contributions

WGB conceived the study; NDW led the mathematical analysis and the numerical modelling; all authors contributed to the
 scenario descriptions and consideration of the modelling results; NDW and WGB drafted the manuscript; all authors reviewed
 the manuscript.

Acknowledgments

We acknowledge funding from the UK EPSRC Global Challenges Research Fund (UCL/BEAMS EPSRC GCRF award
 172313) to WGB for research on *Poroelasticity in the Bengal Aquifer System and groundwater resources monitoring in*
Bangladesh. NDW thanks the University of Southampton for leave of absence during the course of the project. Field
 measurements at Khulna and Laksmipur were made with the kind assistance of the Bangladesh Water Development Board
 (BWDB) and financial support from the UK Department for International Development (DfID) under the project *Groundwater*
Resources in the Indo-Gangetic Basin (Grant 202125-108) managed by Professor Alan MacDonald of the British Geological
 Survey. We are grateful to Professors Mike Steckler, Columbia University, and Humayun Akhter, Dhaka University, for useful
 discussions on ground surface vertical motions in the Bengal Basin, and to John Barker and William Powrie for helpful
 discussion of the fundamental processes at the start of the research. Dr. Mohammed Shamsudduha, University College
 London, and Ms. Sarmin Sultana, Dhaka University are thanked for discussions on the hydrological context of the groundwater
 level monitoring piezometers. The data used are listed in the references and illustrated in the Supplementary Information.

Nomenclature

α	Proportion of mechanical load as head
α_B	Biot-Willis coefficient, $1 - K/K_s$
β, C	3D loading efficiency, Skempton's coefficient, or 'tidal efficiency'
δ_{ij}	Kronecker delta
ε_{ij}	Strain
θ	$z \sqrt{\frac{\omega}{2D}} = z \sqrt{\frac{\pi}{DT}}$



580	λ	$2\alpha_B(1 - 2\nu)/3(1 - \nu)$
581	ν	Poisson's ratio
582	ξ	1D loading efficiency
583	κ	Hydraulic conductivity
584	ρ	Water density
585	σ_{ij}	Stress tensor
586	σ_t	Total stress
587	ψ	Lag (radians)
588	ω	Angular frequency
589		
590	a	River half-width
591	B	Barometric efficiency
592	E	Young's Modulus
593	D	Hydraulic diffusivity
594	g	Acceleration due to gravity
595	G	Shear Modulus
596	h	Head
597	$H(t)$	Top boundary head
598	H_0	Amplitude of top boundary head
599	J	Fluid source term
600	K	Bulk Modulus of porous medium
601	K_f	Bulk modulus of the water
602	K_s	Bulk modulus of the solid grains
603	$L(t)$	Top boundary load
604	L_0	Amplitude of top boundary load
605	n	Porosity
606	p	Pore pressure
607	S_y	Specific Yield
608	S_s	Specific storage
609	S_{s3}	3D Specific storage
610	t	Time
611	u	Vertical displacement
612	x	Perpendicular distance from a river



613 z Vertical coordinate

614

615 References

616

- 617 COMSOL Multiphysics® v. 5.2. www.comsol.com. . COMSOL AB, Stockholm, Sweden.
- 618 Acworth, R. I., Rau, G. C., McCallum, A. M., Andersen, M. S., and Cuthbert, M. O.: Understanding connected surface-
 619 water/groundwater systems using Fourier analysis of daily and sub-daily head fluctuations, *Hydrogeology Journal*, 23, 143-
 620 159, 2015.
- 621 Bakker, M.: The effect of loading efficiency on the groundwater response to water level changes in shallow lakes and
 622 streams, *Water Resources Research*, 52, 1075-1715, 2016.
- 623 Bardsley, W. E. and Campbell, D. J.: An expression for land surface water storage monitoring using a two-formation
 624 geological weighing lysimeter, *Journal of Hydrology*, 335, 240-246, 2007.
- 625 Bardsley, W. E. and Campbell, D. J.: Natural geological weighing lysimeters: calibration tools for satellite and ground
 626 surface gravity monitoring of subsurface water-mass change, *Natural Resources Research*, 9, 147-156, 2000.
- 627 Bardsley, W. E. and Campbell, D. J.: A new method for measuring near-surface moisture budgets in hydrological systems,
 628 *Journal of Hydrology*, 154, 245-254, 1994.
- 629 Barr, A. G., van der Kamp, G., Schmidt, R., and Black, T. A.: Monitoring the moisture balance of a boreal aspen forest using
 630 a deep groundwater piezometer, *Agricultural and Forest Meteorology*, 102, 13-24, 2000.
- 631 Benner, S. G., Polizzotto, M. L., Kocar, B. D., Ganguly, S., Phan, K., Ouch, K., Sampson, M., and Fendorf, S.: Groundwater
 632 flow in an arsenic-contaminated aquifer, Mekong Delta, Cambodia, *Applied Geochemistry*, 23, 3072-3087, 2008.
- 633 Bense, V. F. and Person, M. A.: Transient hydrodynamics within intercratonic sedimentary basins during glacial cycles,
 634 *Journal of Geophysical Research:Earth Surface* (2003-2012), 113, 2008.
- 635 Black, J. H. and Barker, J. A.: The puzzle of high heads beneath the West Cumbrian coast, UK: a possible solution,
 636 *Hydrogeology Journal*, 24, 439-457, 2016.
- 637 Boutt, D. F.: Poroelastic loading of an aquifer due to upstream dam releases, *Ground Water*, 48, 580-592, 2010.
- 638 Burbey, T. J., Warner, S. M., Blewitt, G., Bell, J. W., and Hill, E.: Three-dimensional deformation and strain induced by
 639 municipal pumping, part 1: Analysis of field data, *Journal of Hydrology*, 319, 123-142, 2006.
- 640 Burgess, W. G., Hoque, M. A., Michael, H. A., Voss, C. I., Breit, G. N., and Ahmed, K. M.: Vulnerability of deep
 641 groundwater in the Bengal Aquifer System to contamination by arsenic, *Nature Geoscience*, 3, 83-87, 2010.
- 642 Burgess, W. G., Shamsudduha, M., Taylor, R. G., Zahid, A., Ahmed, K. M., Mukherjee, A., and Lapworth, D. J.: Seasonal,
 643 episodic and periodic changes in terrestrial water storage recorded by deep piezometric monitoring in the
 644 Ganges/Brahmaputra/Meghna delta, AGU Fall Meeting 2014, San Francisco, 2014.
- 645 Burgess, W. G., Shamsudduha, M., Taylor, R. G., Zahid, A., Ahmed, K. M., Mukherjee, A., Lapworth, D. J., and Bense, V.
 646 F.: Terrestrial water load and groundwater fluctuation in the Bengal Basin, *Scientific Reports*, 7, 2017.
- 647 BWDB: Establishment of monitoring network and mathematical model study to assess salinity intrusion in groundwater in
 648 the coastal area of Bangladesh due to climate change. Final report. , Bangladesh Water Development Board, Dhaka, 773 pp.,
 649 2013.
- 650 Chaussard, E., Burgmann, R., Shirzaei, M., Fielding, E. J., and Baker, B.: Predictability of hydraulic head changes and
 651 characterization of aquifer-system and fault properties from InSAR-derived ground deformation, *Journal of Geophysical
 652 Research: Solid Earth*, 119, 6572-6590, 2014.
- 653 de Silva, S., Wightman, N. R., and Kamruzzaman, M.: Geotechnical ground investigation for the Padma Main Bridge,
 654 Dhaka, Bangladesh, August 8-10, 2010 2010.
- 655 Domenico, P. A. and Schwartz, F. W.: *Physical and Chemical Hydrogeology*, John Wiley & Sons, New York, 1998.
- 656 Erban, L. E., Gorelick, S. M., and Zebker, H. A.: Groundwater extraction, land subsidence, and sea-level rise in the Mekong
 657 Delta, Vietnam, *Environmental Research Letters*, 9, 2014.



- 658 Fendorf, S., Michael, H. A., and van Geen, A.: Spatial and temporal variations of groundwater arsenic in south and southeast
659 Asia, *Science*, 328, 1123-1127, 2010.
- 660 Gibson, R. E.: The analytical method in soil mechanics, *Geotechnique*, 24, 115-140, 1974.
- 661 Green, D. H. and Wang, H. F.: Specific storage and poroelastic coefficient, *Water Resources Research*, 26, 1631-1637, 1990.
- 662 Hoque, M. A., Burgess, W. G., and Ahmed, K. M.: Integration of aquifer geology, groundwater flow and arsenic distribution
663 in deltaic aquifers – A unifying concept, *Hydrological Processes*, 31, 2095-2109, 2017.
- 664 Hussain, M. M. and Abdullah, S. K. M.: Geological setting of the areas of arsenic safe aquifers. Report of the ground water
665 task force, Ministry of Local Government, Rural Development & Cooperatives, Local Government Division,
666 Bangladesh Interim Report No. 1, 2001.
- 667 Jacob, C. E.: On the flow of water in an elastic artesian aquifer, *Transactions of the American Geophysical Union*, 1940.
668 574-586, 1940.
- 669 Lambert, A., Huang, J., van der Kamp, G., Henton, J., Mazzotti, S., James, T. S., Courtier, N., and Barr, A. G.: Measuring
670 water accumulation rates using GRACE data in areas experiencing glacial isostatic adjustment: The Nelson River basin,
671 *Geophysical Research Letters*, 40, 6118-6122, 2013.
- 672 Larsen, F., Pham, N. Q., Dang, N. D., Postma, D., Jessen, S., Pham, V. H., Nguyen, T. B., Trieu, H. D., Tran, L. T., Nguyen,
673 H., Chambon, J., Nguyen, H. V., Ha, D. H., Hue, N. T., Duc, M. T., and Refsgaard, J. C.: Controlling geological and
674 hydrogeological processes in an arsenic contaminated aquifer on the Red River flood plain, Vietnam, *Applied Geochemistry*,
675 23, 3099-3115, 2008.
- 676 Manga, M. I., Beresnev, I., Brodsky, E. E., Elkhoury, J. E., Elsworth, D., Ingebritsen, S. E., Mays, D. C., and Wang, C.-Y.:
677 Changes in permeability caused by transient stresses: field observations, experiments, and mechanisms, *Reviews of*
678 *Geophysics*, 50, 2012.
- 679 Marin, S., van der Kamp, G., Pietroniro, A., Davison, B., and Toth, B.: Use of geological weighing lysimeters to calibrate a
680 distributed hydrological model for the simulation of land-atmosphere moisture exchange, *Journal of Hydrology*, 383, 179-
681 185, 2010.
- 682 Michael, H. A. and Voss, C. I.: Controls on groundwater flow in the Bengal Basin of India and Bangladesh: regional
683 modeling analysis, *Hydrogeology Journal*, 17, 1561-1577, 2009a.
- 684 Michael, H. A. and Voss, C. I.: Estimation of regional-scale groundwater flow properties in the Bengal Basin of India and
685 Bangladesh, *Hydrogeology Journal*, 17, 1329-1346, 2009b.
- 686 Michael, H. A. and Voss, C. I.: Evaluation of the sustainability of deep groundwater as an arsenic-safe resource in the
687 Bengal Basin, *PNAS*, 105, 8531-8536, 2008.
- 688 Mukherjee, A., Fryar, A. E., and Rowe, H. D.: Regional hydrostratigraphy and groundwater flow modeling of the arsenic
689 affected western Bengal basin, West Bengal, India, *Hydrogeology Journal*, 15, 1397-1418, 2007.
- 690 Narasimhan, T. N.: On storage coefficient and vertical strain, *Ground Water*, 44, 488-491, 2006.
- 691 Neuzil, C. E.: Hydromechanical coupling in geological processes, *Hydrogeology Journal*, 11, 41-83, 2003.
- 692 Pacheco, F. A. L. and Fallico, C.: Hydraulic head response of a confined aquifer influenced by river stage fluctuations and
693 mechanical loading, *Journal of Hydrology*, 531, 716-727, 2015.
- 694 Powrie, W.: *Soil Mechanics: Concepts and Applications*, CRC Press, Taylor and Francis Group, Boca Raton, Florida, 2014.
- 695 Rahman, M. A. T., Majumder, R. K., Rahman, S. H., and Halim, M. A.: Sources of deep groundwater salinity in the
696 southwestern zone of Bangladesh, *Environmental Earth Sciences*, 63, 363-373, 2011.
- 697 Ravenscroft, P., Burgess, W. G., Ahmed, K. M., Burren, M., and Perrin, J.: Arsenic in groundwater of the Bengal Basin,
698 Bangladesh: Distribution, field relations, and hydrogeological setting, *Hydrogeology Journal*, 13, 727-751, 2005.
- 699 Ravenscroft, P., McArthur, J. M., and Hoque, M. A.: Stable groundwater quality in deep aquifers of Southern Bangladesh:
700 The case against sustainable abstraction, *Sci Total Environ.*, 454-455, 627-638, 2013.
- 701 Reeves, J. A., Knight, R., Zebker, H. A., Kitanidis, P. K., and Schreuder, W. A.: Estimating temporal changes in hydraulic
702 head using InSAR data in the San Luis Valley, Colorado, *Water Resources Research*, 50, 4459-4473, 2014.
- 703 Roeloffs, E. A.: Fault stability changes induced beneath a reservoir with cyclic variations in water level, *Journal of*
704 *Geophysical Research*, 93, 2107-2124, 1988.
- 705 Rojstaczer, S. and Agnew, D. C.: The influence of formation material properties on the response of water levels in wells to
706 Earth tides and atmospheric loading, *Journal of Geophysical Research*, 94, 12,403-412, 1989.



- 707 Shamsudduha, M., Taylor, R. G., Ahmed, K. M., and Zahid, A.: The impact of intensive groundwater abstraction on
708 recharge to a shallow regional aquifer system: evidence from Bangladesh, *Hydrogeology Journal*, 19, 901-916, 2011.
- 709 Shamsudduha, M., Taylor, R. G., Chandler, R. E., and Ahmed, K. M.: Basin-scale variations in shallow groundwater levels
710 in Bangladesh over the last 40 years: assessing the impacts of groundwater-fed irrigation. In: *Water scarcity and water*
711 *security seminar*, Geological Society, London, U. K., 2008.
- 712 Shamsudduha, M., Taylor, R. G., and Longuevergne, L.: Monitoring groundwater storage changes in the highly seasonal
713 humid tropics: validation of GRACE measurements in the Bengal Basin, *Water Resour. Res.*, doi: 10.1029/2011WR010993,
714 2012. W02508, 2012.
- 715 Smith, C., van der Kamp, G., Arnold, L., and Schmidt, R.: Measuring precipitation with a geolysimeter, *Hydrology and Earth*
716 *System Science*, 21, 5263–5272, 2017.
- 717 Steckler, M. S., Nooner, S. L., Akhter, S. H., Chowdhury, S. K., Bettadpur, S., Seeber, L., and Kogan, M. G.: Modeling earth
718 deformation from monsoonal flooding in Bangladesh using hydrographic, GPS and GRACE Data, *Journal of Geophysical*
719 *Research*, 115, 2010.
- 720 Sultana, S., Ahmed, K. M., Mahtab-Ul-Alam, S. M., Hasan, M., Tuinhof, A., Ghosh, S. K., Rahman, M. S., Ravenscroft, P.,
721 and Zheng, Y.: Low-cost aquifer storage and recovery: implications for improving drinking water access for rural
722 communities in coastal Bangladesh, *Journal of Hydrologic Engineering*, 20, B5014007-5014001-5014012, 2015.
- 723 Sutherland, R., Townend, J., Toy, V., Upton, P., Coussens, J., Allen, M., and etc.: Extreme hydrothermal conditions at an
724 active plate-bounding fault, *Nature*, 546, 137-140, 2017.
- 725 Tam, V. T., Batelaan, O. L. T. T., and Nhan, P. Q.: Three-dimensional hydrostratigraphical modelling to support evaluation
726 of recharge and saltwater intrusion in a coastal groundwater system in Vietnam, *Hydrogeology Journal*, 22, 1749-1762,
727 2014.
- 728 Tapley, B. D., Bettadpur, S., Ries, J. C., Thompson, P. F., and Watkins, M. M.: GRACE measurements of mass variability in
729 the Earth system, *Science*, 305, 503-505, 2004.
- 730 Tiwari, V. M., Wahr, J., and Swenson, S.: Dwindling groundwater resources in northern India, from satellite gravity
731 observations, *Geophys. Res. Lett.*, 36, L18401, 2009.
- 732 van der Kamp, G. and Gale, J. E.: Theory of Earth tide and barometric effects in porous formations with compressible grains,
733 *Water Resources Research*, 19, 538-544, 1983.
- 734 van der Kamp, G. and Maathuis, H.: Annual fluctuations of groundwater levels as a result of loading by surface moisture,
735 *Journal of Hydrology*, 127, 137-152, 1991.
- 736 van der Kamp, G. and Schmidt, R.: Monitoring of total soil moisture on a scale of hectares using groundwater peizometers,
737 *Geophysical Research Letters*, 24, 719-722, 1997.
- 738 van der Kamp, G. and Schmidt, R.: Review: Moisture loading - the hidden information in groundwater observation well
739 records, *Hydrogeology Journal*, 25, 2225-2233, 2017.
- 740 Verruijt, A.: Elastic storage of aquifers. In: *Flow through porous media*, Weist, R. J. M. d. (Ed.), Academic Press Inc., New
741 York, 1969.
- 742 Xu, X., Huang, G., Qu, Z., and Pereira, L. S.: Using MODFLOW and GIS to assess changes in groundwater dynamics in
743 response to water saving measures in irrigation districts of the Upper Yellow River Basin, *Water Resources Management*,
744 25, 2035-2059, 2011.

745

746